A Dual Barcoding Approach to Bacterial Strain Nomenclature: Genomic Taxonomy of Klebsiella pneumoniae Strains

Melanie Hennart, Julien Guglielmini, Sébastien Bridel, Martin C J Maiden, Keith A. Jolley, Alexis Criscuolo, Sylvain Brisse

A dual barcoding approach to bacterial strain nomenclature: Genomic taxonomy of *Klebsiella pneumoniae* strains

Melanie Hennart [a,b], Julien Guglielmini [c], Sébastien Bridel [a], Martin C.J. Maiden [d], Keith A. Jolley [d], Alexis Criscuolo [c] and Sylvain Brisse [a]

Affiliations:

[a] Institut Pasteur, Université Paris Cité, Biodiversity and Epidemiology of Bacterial Pathogens, F-75015, Paris, France

[b] Sorbonne Université, Collège doctoral, F-75005 Paris, France

[c] Institut Pasteur, Université Paris Cité, Bioinformatics and Biostatistics Hub, F-75015 Paris, France

[d] Department of Zoology, University of Oxford, 11a Mansfield Road, Oxford, OX1 3SZ, United Kingdom

***Correspondence**:

Sylvain Brisse. Institut Pasteur, Biodiversity and Epidemiology of Bacterial Pathogens, F-75724 Paris, France. E-mail: sylvain.brisse@pasteur.fr; Tel: +33 1 45 68 83 34

Keywords: genomic classification, strain nomenclature, microevolution, pathogen tracking, genomic library, international harmonization

Running Title: *Klebsiella* strain taxonomy

Abstract

Sublineages within microbial species can differ widely in their ecology and pathogenicity, and their precise definition is important in basic research and for industrial or public health applications. Widely accepted strategies to define sublineages are currently missing, which confuses communication in population biology and epidemiological surveillance.

Here we propose a broadly applicable genomic classification and nomenclature approach for bacterial strains, using the prominent public health threat *Klebsiella pneumoniae* as a model. Based on a 629-gene core genome multilocus sequence typing (cgMLST) scheme, we devised a dual barcoding system that combines multilevel single linkage (MLSL) clustering and life identification numbers (LIN). Phylogenetic and clustering analyses of >7,000 genome sequences captured population structure discontinuities, which were used to guide the definition of 10 infra-specific genetic dissimilarity thresholds. The widely used 7-gene multilocus sequence typing (MLST) nomenclature was mapped onto MLSL sublineages (threshold: 190 allelic mismatches) and clonal group (threshold: 43) identifiers for backwards nomenclature compatibility. The taxonomy is publicly accessible through a community-curated platform (https://bigsdb.pasteur.fr/klebsiella), which also enables external users' genomic sequences identification.

The proposed strain taxonomy combines two phylogenetically informative barcode systems that provide full stability (LIN codes) and nomenclatural continuity with previous nomenclature (MLSL). This species-specific dual barcoding strategy for the genomic taxonomy of microbial strains is broadly applicable and should contribute to unify global and cross-sector collaborative knowledge on the emergence and microevolution of bacterial pathogens.

Introduction

Taxonomy is a foundation of biology that entails the classification, nomenclature, and identification of biological objects (Cowan 1965). Although the Linnaean system is organized into taxonomic ranks down to the level of species (Sneath 1992), sublineages within microbial species can diversify as independently evolving lineages that persist over long periods of time, (Selander and Levin 1980) and the broad microbial species definition and horizontal gene transfer of accessory genes underlie extensive strain heterogeneity of phenotypes with ecological, medical or industrial relevance (Hacker and Kaper 2000; Lan and Reeves 2001; Feil 2004; Konstantinidis and Tiedje 2005). Nevertheless, strain-level diversity is overlooked by current prokaryotic taxonomy.

Most attempts to develop and maintain microbial strain taxonomies aimed at facilitating epidemiological surveillance and outbreak detection (Maiden et al. 1998; van Belkum et al. 2007; Maiden et al. 2013). Although local epidemiology can rely on vernacular type designations, the benefits of unified nomenclatures of sublineages for large-scale epidemiology and population biology were recognized early (Struelens, De Gheldre, and Deplano 1998). By far the most successful taxonomic system of microbial strains is the multilocus sequence typing (MLST) approach (Maiden et al. 1998; Achtman et al. 2012). This highly reproducible and portable nomenclature system has been extensively used for studies of population biology and public health surveillance of bacterial pathogens (Keith A. Jolley, Bray, and Maiden 2018). Core genome MLST (cgMLST) extends the advantages of the MLST approach at the genomic scale (K. A. Jolley and Maiden 2010; Maiden et al. 2013) and provides strain discrimination at much finer scales.

Strain classification, based either on cgMLST or on nucleotide polymorphisms, can be achieved by using several clustering thresholds simultaneously, leading to a succession of group identifiers ('barcodes') that provide relatedness information at increasing levels of phylogenetic depth (Maiden et al. 2013; Moura et al. 2016). This approach was recently formalized as hierarchical clustering (HierCC, based on cgMLST) (Zhou, Charlesworth, and Achtman 2021) and as the 'single nucleotide polymorphism (SNP) address' (Dallman et al. 2018) , based on single linkage classifications; here we generically refer to these approaches as MultiLevel Single Linkage (MLSL). Unfortunately, the single linkage clustering may result in the fusion of preexisting groups as additional genomes are introduced, due to the possibility of new genomes being less distant than the threshold, from two distinct groups. This approach thus suffers from instability, which led HierCC inventors to instead use *ad-hoc* group attribution rules after an initial single linkage classification (Zhou, Charlesworth, and Achtman 2021).

An alternative approach, the Life Identification Number (LIN) encoding, was proposed by Vinatzer and colleagues (Vinatzer, Tian, and Heath 2017; Tian et al. 2020): a multi-position numerical code is assigned to each genome based on its similarity with the closest genome already encoded. An attractive property of this procedure is that LIN codes are definitive, *i.e*., not affected by subsequent additions of genomes, as they are attributed to individual genomic sequences rather than to groups. However, in the current implementation of LIN codes the similarity between genomes is estimated using Average Nucleotide Identity (ANI), which may be imprecise for nearly identical strains.

Here, we present a strain classification, naming and identification system for bacterial strains, which is based on cgMLST and combines the MLSL and LIN code approaches. We took as a model the *Klebsiella pneumoniae* species complex, a genetically and ecologically highly diverse bacterial group that causes a wide range of infections in humans and animals (Brisse, Grimont, and Grimont 2006; Wyres, Lam, and Holt 2020). Given its extensive diversity and fast evolutionary dynamics, *K. pneumoniae* is a challenging model for the development of a genomic taxonomy of strains. Moreover, the rapid emergence and global dissemination of multidrug resistance in *K. pneumoniae,* sometimes combined with high virulence, (Bialek-Davenet et al. 2014; Wyres et al. 2020) have created a pressing need for an efficient *K. pneumoniae* strain definition and tracking system.

Results

Genome-based phylogenetic structure of the K. pneumoniae species complex (KpSC)

The deep phylogenetic structure of the *K. pneumoniae* (Kp) species complex (**Figure 1**) reflects the previously recognized seven major phylogroups, Kp1 to Kp7 (Brisse and Verhoef 2001; Fevre et al. 2005; Blin et al. 2017; Long et al. 2017; Rodrigues et al. 2019; Wyres, Lam, and Holt 2020). The most represented phylogroup (91.7%; n=6,476) is Kp1, *i.e.*, *K. pneumoniae sensu stricto* (**Table 1**), and its phylogenetic structure (**Figure 2**) revealed a multitude of sublineages (note that below, we define sublineages and clonal groups is a stricter sense in paragraph "Definition of classification thresholds for phylogroups, sublineages and clonal groups"). There were multiple closely-related isolates within some sublineages, most prominently within a sublineage comprising genomes with 7-gene MLST identifiers ST258, ST11, ST512 (**Figure 2**), which represented more than a third (33.4%) of the Kp1 dataset. The abundance of this sublineage (and a few others, such as ST23) reflected the clinical microbiology focus on multidrug resistant or hypervirulent isolates (Bowers et al. 2015; Struve et al. 2015; Lam et al. 2018; Wyres et al. 2020). The phylogenetic structure within other *K. pneumoniae* phylogroups also revealed a multitude of distinct sublineages but no predominant ones, and medically important lineages in these phylogroups are yet to be recognized.

K. pneumoniae strains can recombine large sections of their chromosome (Chen et al. 2014; Wyres et al. 2015). Large recombination events were detected in 1.9% (138/7,198) genomes (based on their cgMLST profiles) and involved the phylogroups Kp1, Kp2 and Kp4 (supplementary appendix: Detection of hybrids**; Figure S1; Table S1; Table S2**). The phylogenetic impact of large-scale recombination is illustrated on **Figure 1**, with 'hybrids' occurring on misleadingly long branches.

cgMLST analysis of the K. pneumoniae species complex

A previously defined core genome MLST (named scgMLST, with 634 loci) scheme (Bialek-Davenet et al. 2014) was updated (**Table S3**) and defined as scgMLSTv2 (with 629 loci, as five of the original ones were removed; see Methods). cgMLST allelic profiles were then determined for 7,433 genomic sequences (including 45 reference sequences; **Figure S2**). The mean number of missing alleles per profile was 8 (1.2%; standard deviation: 25; 4.0%), and most (7,198; 96.8%) isolates had a cgMLST profile with fewer than 30 (4.8%) missing alleles. Missing allele proportions did not vary significantly among phylogroups (**Table 1**). The transcription-repair coupling factor *mfd* gene was atypical, with 778 alleles and an average allele size of 3,447 nucleotides (nt); for the other loci, the number of distinct alleles varied from 8 to 626 (median: 243), and was strongly associated with locus size (range: 123 to 2,826 nt; median: 758 nt; **Figure S3**). Locus-by-locus recombination analyses detected evidence of intra-gene recombination (PHI test; 5% *p*-value significance) in half of the loci (318/629; 50.6%) and these exhibited more alleles than non-recombining ones (**Table S3; Figure S3**).

The distribution of pairwise allelic mismatch proportions among non-hybrid cgMLST allelic profiles was discontinuous (**Figure 3**), with four major modes centered around values 99.7% (627 mismatches; *i.e.*, 0.3% similarity), 82.7% (520 mismatches; 17.3%), 12.4% (79 mismatches; 87.6%) and 2.0% (13 mismatches; 98%). Average nucleotide identity (ANI) values (**Figure S4**) varied from 92.8% to 100%, with two first modes at 93.5% and 95.5%, composed of inter-phylogroup strain comparisons. The corresponding genome pairs typically had only ≈2% cgMLST similarity. In turn, whereas the range of ANI values was only 98% to 100% for intra-species pairs, their cgMLST similarities occupied the much broader 5%-100% range.

The 627-mismatch mode corresponded mostly to pairs of strains belonging to distinct species of the KpSC (**Figure 3; Figure S4**), while a minor peak centered on 591 mismatches (**Figure S5**) corresponded to comparisons between subspecies of *K. quasipneumoniae* and *K. variicola* (Kp2 and Kp4, and Kp3 and Kp5, respectively; **Figure S4**). Whereas the 520-mismatch mode corresponded to inter-ST comparisons in 99.9% cases, the 13-mismatch mode was largely dominated by comparisons of cgMLST profiles with the same ST (68.2%; pairs of genomes within 402 distinct STs) or of single-locus variants (SLV; 30.8%). Finally, the 79-mismatch mode comprised a large proportion (48.0%) of ST258-ST11 comparisons and other comparisons of atypically closely-related STs (**Figure S5**).

Definition of classification thresholds for phylogroups, sublineages and clonal groups

To determine optimal allelic mismatch thresholds that would reflect the KpSC population structure, the consistency and stability properties of single linkage clustering groups were assessed for every threshold value t from 1 to 629 allelic mismatches. The consistency (silhouette) coefficient S_t had a plateau of optimal values in the range corresponding to 118/629 (18.8%) to 355/629 (56.4%) allelic mismatches (**Figure 3, blue curve**). Analysis of the robustness to subsampling (W_t; based on an adjusted Wallace coefficient; **Figure 3, green curve**) identified several ranges of allelic mismatch threshold values that were associated to maximal stability.

The above analyses led us to propose four deep classification levels. The two first thresholds, 610 and 585 allelic mismatches, enable species and subspecies separations, respectively. We next defined a threshold of 190 allelic mismatches, corresponding to the optimal combination of consistency and stability coefficients S_t and W_t. The single linkage clustering based on this threshold created 705 groups, which we here define as 'sublineages' (SL). By design, this threshold separated into distinct groups, the pairs of cgMLST profiles corresponding to the major mode (at 520 mismatches), *i.e.*, the majority of genomes that have distinct STs within phylogroups. Finally, a threshold of 43 allelic mismatches was defined to separate genome pairs of the 79-mismatch mode. This value corresponded to local optima of both S_t and W_t coefficients. Interestingly, this last threshold value was also located in the optimal range of compatibility with the classical 7-gene ST definitions (Rand index $R_t \geq 0.70$ was observed for $10 \leq t \leq 51$). The use of this threshold resulted in 1,147 groups, which we propose to define as 'clonal groups' (CG).

Overall, approximately half (547/1,147; 47.7%) of the CGs corresponded one-to-one with the sublineage level (**Table S4**): 77.6% (547/705) sublineages contained a single CG, whereas 158 (22.4%) sublineages comprised at least two clonal groups (**Table S5; Figure 4; Figure S6**). Overall, CG compatibility with classical ST classification was high (*i.e.*, R_t = 0.72, whereas it was only 0.50 for sublineages).

The distribution of pairwise allelic mismatch values that involved hybrid genomes showed an additional peak around 39 shared alleles (*i.e.*, 590 allelic mismatches; **Figure S7**). Therefore, these inter-phylogroup hybrids were placed into distinct partitions at the 585-mismatch level. However, as some of these hybrid genomes diverged by fewer than 585 allelic mismatches from two distinct phylogroups at the same time, they would cause fusion of phylogroup partitions upon single linkage clustering. To highlight the impact of this phenomenon, hybrids were first filtered out, and next incorporated in a second single linkage clustering step (supplementary appendix; **Figure S8**).

Phylogenetic compatibility of sublineages and clonal groups

To estimate the congruence of classification groups with phylogenetic relationships among genomic sequences, we quantified the proportion of monophyletic (single ancestor, exclusive group), paraphyletic (single ancestor, non-exclusive group) and polyphyletic (two or more distinct ancestors) groups. Regarding 7-gene MLST, 6,985 (98.9%) genomes had a defined ST, *i.e.,* an allele was called for each of the seven genes. Of the 992 distinct STs, 396 were non-singleton STs (*i.e.*, comprised at least two isolates). Of these, 286 (72.2%) were monophyletic, nine were paraphyletic (2.3%) and 101 (25.5%) were polyphyletic. The monophyletic STs comprised only 22% of all genomes in non-singleton STs.

Regarding cgMLST-based classification, there were five and seven partitions at 610 and 585 allelic mismatch levels, respectively, and 100% of these were monophyletic. Among the 705 distinct sublineages (SLs), 317 (45.0%) were non-singleton, and most (310; 97.8%) of these were monophyletic (**see Figure 2 for Kp1**); only three (0.9%) were paraphyletic, and four (1.3%) were polyphyletic (**Table S4**). The monophyletic SLs comprised a large majority (5,961/6,672; 89.3%) of genomes in non-singleton STs.

Finally, 396 out of 1,147 (34.5%) clonal groups (CGs) were non-singleton; most (362; 91.4%) were monophyletic (**Figure 2**), whereas eight (2.0%) were paraphyletic, and 26 (6.6%) were polyphyletic (**Table S5**). Monophyletic CGs comprised nearly half (3,030; 48.0%) of the genomes in the non-singleton CGs, whereas 3,224 (51.1%) were in polyphyletic groups, mostly in CG258, CG340 and CG15.

Definition of shallow-level classification thresholds for Klebsiella epidemiology

Although the scgMLSTv2 scheme comprises only 629 loci, or ~10% of a typical *K. pneumoniae* genome length (512,856 nt out of 5,248,520 in the NTUH-K2044 genome), shallow-level classifications of genomic sequences might be useful for tentative outbreak delineation and epidemiological surveillance purposes, by ruling-out outliers. To provide flexible case cluster definitions, we classified KpSC cgMLST profiles using thresholds of 0, 1, 2, 4, 7 and 10 scgMLSTv2 allelic mismatches. Together with the four higher levels, the MLSL nomenclature therefore comprises 10 classification levels in total. The classification groups corresponding to the 0-mismatch threshold correspond to groups of cgST profiles that only differ by missing data. We observed that profiles of isolates involved in previously reported KpSC outbreaks generally differed by no or 1 mismatch, with a maximum of five allelic mismatches (**Table S6**; **Table S7**), indicating that this classification approach may be useful for genomic surveillance and outbreak identification purposes.

Inheritance of the 7-gene ST identifiers into the cgMLST classification, and characteristics of main sublineages (SLs) and clonal groups (CGs)

To attribute SL and CG identifiers that corresponded maximally to the widely adopted 7-gene ST identifiers, we developed an inheritance algorithm to map MLST identifiers onto SL and CG partitions (see supplementary appendix: Nomenclature inheritance algorithm). Of the 705 SLs, most (683; 96.9%) were named by inheritance and this was the case for 879 (76.6%) of the 1,047 CGs (**Table S4**). The resulting correspondence of cgMLST partitions with classical MLST was evident for the major groups

(**Figure 4; Figure S6**). For instance, the multidrug resistant SL258 comprised isolates belonging to MLST sequence types ST258, ST11, ST512, ST340, ST437 and 25 other STs. SL258 consisted of 16 distinct CGs, of which the four most frequent were defined as CG258 (61.2%), CG340 (17.8%), CG11 (17.3%) and CG3666 (2.8%) (**Figure 4**). When compared to 7-gene MLST, most isolates of CG258 were ST258 (75.6%) or ST512 (22.6%), whereas CG11 mostly comprised ST11 genomes (98.0%). In turn, CG340 included a large majority of ST11 genomes (61.8%) and only 20.0% ST340 genomes, and was named CG340 rather than CG11 because CG11 was already attributed. Likewise, the majority (83/86; 96.5%) of ST23 genomes, which are associated with pyogenic liver abscess (Lam et al. 2018), were classified into SL23, which itself consisted mainly (84/90, 93.3%) of ST23 genomes (**Figure 4**). The well-recognized emerging multidrug resistant KpSC populations of ST15, ST101, ST147 and ST307 each corresponded largely to a single SL and CG (**Figure S6**).

The frequency of detection of virulence and antimicrobial resistance genes differed among the main SLs and CGs (**Figure 5; Figure S9**). As expected (Lam et al. 2021), SL23 (median virulence score of 5) and SL86 (median score 3) were prominent 'hypervirulent' sublineages, and they were largely lacking resistance genes. In contrast, a majority of strains from SLs 258, 147, 101, 307 and 37, as well as a large number of other SLs, had a resistance score of 2 or more, indicative of BLSE/carbapenemases, but these had modest virulence scores (**Figure S9**). SL231 genomes stood out as combining high virulence and resistance scores. In some cases, CGs within single major SLs had contrasted virulence and resistance gene contents (**Figure 6**).

Development and implementation of a cgMLST-based LIN code system

Following the principle of the LIN code system, initially proposed based on the ANI similarity (Marakeby et al. 2014), we defined a cgMLST-based LIN (cgLIN) code approach. As LIN coding is performed sequentially, we first explored the impact on the resulting partitioning of cgMLST profiles, of the order in which genomes are assigned. We confirmed that the number of partitions (hence their content too) varied according to input order (**Figure S10**). However, we established that the order of genomes determined by the traversal of a Minimum Spanning tree (MStree) (Prim 1957, 57) naturally induces a LIN encoding order that is optimal, *i.e.,* most parsimonious with respect to the number of identifiers generated at each position of the code (see supplementary appendix). Using this MStree traversal strategy, we defined cgLIN codes for the 7,060 non-hybrid genomes (as a first step), resulting in 4,889 distinct cgLIN codes.

Furthermore, cgLIN codes can be displayed in the form of a prefix tree (**Figure 5**), which largely reflects the phylogenetic relationships among genomes. In addition, cgLIN code prefixes can be used to label particular phylogenetic lineages (Vinatzer, Tian, and Heath 2017). For example, a single cgLIN code prefix defined each phylogroup (*e.g.*, Kp1: prefix 0_0; Kp2: prefix 2_0; **Figure 5**). Likewise, a full one-to-one correspondence between prefixes and SLs was observed, and almost all (99.4%) CGs also had a unique prefix (**Table S4; Table S5; Figure 6).**

Effect of hybrid genomes incorporation on the MLSL and cgLIN codes classifications

Because inter-phylogroup hybrid genomes have smaller distances to their parental phylogroups than the inter-phylogroup distances resulting from vertical evolutionary events, their incorporation into the MLSL classification may induce fusion of previously distinct single linkage groups. To illustrate this chaining effect, the 'hybrid' genomes were included into the MLSL nomenclature in a second step, and fusions of previously existing partitions we recorded; for example, at the 610 allelic mismatch threshold, partitions 2 (Kp2 and Kp4) and 4 (Kp3 and Kp5) were merged with partition 1 (Kp1). At the 585-mismatch threshold, partitions 5 (Kp2) and 2 (Kp4) were merged with partition 1 (Kp1). At the 190-mismatch threshold, only one fusion was observed, between partitions 184 (SL113) and 465 (SL1518; **Figure S11**). The partitions at other thresholds were not impacted by the addition of the hybrid genomes.

In contrast, the incorporation of hybrid genomes into the cgLIN code database left the cgLIN codes of the 7,060 previous genomes entirely unaffected; there were no merging of groups, as per design of the system. In particular, the seven phylogroup prefixes corresponding to species and subspecies remained unaffected (**Figure S11**); instead, additional prefixes were created for the hybrid genomes (**Table S1; Table S2**).

Implementation of the genomic taxonomy in a publicly-accessible database

The MLSL nomenclature was incorporated into the Institut Pasteur *K. pneumoniae* MLST and whole genome MLST databases (https://bigsdb.pasteur.fr/klebsiella) under the classification scheme functionality developed in BIGSdb version 1.21.0. In brief, the cgMLST profile of every isolate with fewer than 30 missing scgMLSTv2 alleles were assigned to a core genome sequence type (cgST), and these were next grouped into single linkage partitions for each of the 10 classification levels. For SLs and CGs, a custom classification group field (named SL or CG within the system) was additionally populated with identifiers inherited from 7-gene MLST. All cgMLST profiles and classification identifiers are publicly available.

To allow users identifying *K. pneumoniae* isolates easily, a profile matching functionality was developed, enabling to search for cgMLST profiles related to a query genome sequence. This was implemented on the website sequence query page (https://bigsdb.readthedocs.io/en/latest/administration.html#scheme-profile-clustering-setting-up-classification-schemes). This functionality returns the classification identifiers (including MLST-inherited CG and SL identifiers) of the cgMLST profile that is most closely related to the query genomic sequence, along with its number of mismatches compared to the closest profile.

cgLIN code functionality was also incorporated into BIGSdb version v1.34.0 (https://bigsdb.readthedocs.io/en/latest/administration.html#setting-up-lincode-definitions-for-cgmlst-schemes). In particular, cgST profiles can be queried by full cgLIN code or any prefix, and a nomenclature can be attached to LINcode prefixes of interest (*e.g.*, SL258 is attached to prefix 0_0_1 and CG258 to 0_0_105_6).

Note that identification of users' query genomic sequences is made possible either through the BIGSdb platform that underlies the cgMLST website, or externally after export of the cgMLST profiles, which are publicly accessible.

Discussion

The existence within microbial species of sublineages with unique genotypic and phenotypic properties underlines the need for infra-specific nomenclatures (Lan and Reeves 2001; Maiden et al. 1998; Rambaut et al. 2020). Similar to species and higher Linnaean taxonomic ranks, a strain taxonomy should: (i) recognize genetic discontinuities and capture the most relevant sublineages at different phylogenetic depths; (ii) provide an unambiguous naming system for sublineages; and (iii) provide identification methods for placement within the taxonomic framework. Here we developed a strain taxonomy consisting of a dual naming system that is grounded in population genetics and linked to an identification tool. The proposed system thus complies with the three fundamental pillars of taxonomy.

Although 7-gene MLST has been widely adopted as a taxonomic system of KpSC strains, several limitations are apparent: besides its restricted resolution, MLST identifiers do not convey phylogenetic information, as a single nucleotide substitution generates a different ST with unapparent relationships with its ancestor. Further, approximately half of the ST partitions were not monophyletic. The cgMLST approach provides much higher resolution and phylogenetic precision (Maiden et al. 2013; Zhou, Charlesworth, and Achtman 2021). Although other metrics such as whole-genome single nucleotide polymorphisms (SNPs) or average nucleotide identity (ANI) can be used to classify strains (Marakeby et al. 2014; Dallman et al. 2018), cgMLST presents advantages inherited from classical MLST, including standardization, reproducibility, portability and the conversion of sequences into human-readable allelic numbers. The high reproducibility and easy interpretation of cgMLST are two critical characteristics for its adoption in epidemiological surveillance. Here, we showed that cgMLST, based on 629 genes, has a much broader dynamic range than ANI when considering intra-specific variation (**Figure S4**), and enables defining several hierarchical classification levels (Zhou, Charlesworth, and Achtman 2021). The resolutive power of the 629-loci cgMLST scheme provides valuable genotyping discrimination up to outbreak resolution and is highly consistent with whole-genome SNPs (Miro et al. 2020). However, to define shallower genetic structure within sublineages resulting from recent clonal expansions or outbreaks, higher resolution should be sought based *e.g.,* on core gene sets of specific sublineages.

Optimization of threshold definitions based on population structure aims at optimizing cluster stability (Barker et al. 2018; Zhou, Charlesworth, and Achtman 2021). The density distribution of pairwise allelic mismatch dissimilarities within *K. pneumoniae* and related species exhibited genetic discontinuities at several phylogenetic depths. We took the benefit of this multimodal distribution to define optimal intra-specific classification thresholds, and combined a clustering consistency coefficient (Silhouette) with a newly developed strategy that evaluates cluster stability by subsampling the entire dataset. We defined four classifications at phylogenetic depths that reflected natural discontinuities within the population structure of *K. pneumoniae*, including the deep subdivisions of *K. pneumoniae sensu lato*. The 190-mismatch sublineage level was designed to capture the numerous deep phylogenetic branches within phylogroups (Bialek-Davenet et al. 2014; Holt et al. 2015). In turn, the clonal group (CG) level was useful to capture the genetic structuration observed within these primary sublineages. For example, the CG-level nomenclature captures the evolutionary split of CG258 and CG11 from their SL258 ancestor, caused by a 1.1 Mb recombination event (Chen et al. 2014) (**Figure S5**).

Seven-locus MLST is a widely adopted nomenclature system, as illustrated by the widespread use of ST identifiers associated with hypervirulent or multidrug resistant sublineages (*e.g.*, '*Klebsiella pneumoniae* ST258': 293 PubMed hits; ST23: 117 hits; on July 20th, 2021). Backward nomenclatural compatibility is therefore critical. After applying our inheritance algorithm, most sublineages and clonal groups were labeled according to the 7-gene MLST identifier of the majority of their isolates. Widely adopted ST identifiers will therefore designate nearly the same strain groups within the proposed genomic taxonomy of *K. pneumoniae*, which should greatly facilitate its adoption. We note that the 7-gene MLST nomenclature will still have to be expanded, as this classical approach continues to be widely used. However, for practical reasons, upcoming MLST and cgMLST nomenclatural identifiers will be uncoupled, and we suggest that the cgMLST-based identifiers of sublineages and clonal groups (rather than their ST) should be adopted as the reference nomenclature in the future.

Instability is a major limitation of single linkage clustering, caused by group fusion known as the chaining effect (Turner and Feil 2007). This is particularly relevant over epidemiological timescales, where intermediate genotypes (*e.g.*, a recent ancestor or recombinant) are often sampled (Feil 2004). This issue is exacerbated in *K. pneumoniae*, where large-scale recombination may result in truly intermediate genotypes (Chen et al. 2014; Holt et al. 2015), referred to as 'hybrids' by analogy to eukaryotic biology. Here this phenomenon was illustrated through our delayed introduction into our nomenclature, of 138 inter-phylogroup hybrid genomes. The merging of predefined classification groups can be handled by classification versioning or *ad hoc* rules (Zhou, Charlesworth, and Achtman 2021), but this is indeterministic and challenging in practice.

To address its stability issue, we complemented the single linkage clustering approach with a fully stable approach. LIN codes were proposed as a universal genome coding system (Marakeby et al. 2014; Tian et al. 2020), a key feature of which is the generation of definitive genome codes that are inherently stable. The original LIN code system was based on the ANI metric; here we noted that the ANI values that best correspond to some of the 10 cgMLST thresholds were highly similar (**Table S8**), casting doubt on the reliability of this metric for small-scale genetic distances. In addition, the ANI metric is non-reciprocal and highly dependent on comparison implementations and parameters. These shortfalls may yield imprecision and non-reproducibility that are particularly impactful for comparisons between very similar genomes. We therefore adapted the LIN code concept to cgMLST-based similarity (*i.e.*, one-complement of the allelic mismatch proportions) to classify strains into a cgLIN code system. This strategy leverages the benefits of cgMLST, and introduces more intuitive shallow-level classification thresholds. The multilevel similarity information embedded in MLSL and cgLIN 'barcodes' provides a human-readable snapshot of strain relationships, as nearly identical genomes have identical barcodes up to a position near the right end. In contrast to single linkage clustering partitions, one important limitation of LIN codes is that preexisting classification identifiers (*e.g.*, ST258) cannot be mapped onto individual LIN code identifiers, because these are attributed with reference to the upper levels and are set to 0 for each downstream level (Marakeby et al. 2014). However, cgLIN code prefixes may represent useful labels for particular lineages.

The cgMLST-based nomenclatures have some limitations. First, comparison of allele numbers rather than SNPs implies loss of information. In turn, this approach is advantageous to estimate evolutionary relationships of closely related genomes that diverged following homologous recombination events, which are common among strains within bacterial species (Feil 2004; Vos and Didelot 2009). Second, MLST-based distances saturate more rapidly than SNP distances (once a locus is affected, even by a single mutation, further mutations at this locus will change the allele but will not increase the allelic distance), and are therefore mostly meaningful within bacterial species. Third, in contrast to the original ANI-based LIN code approach (Tian et al. 2020), cgMLST-based LIN codes require prior development of cgMLST schemes, which are larger, hence more powerful for strain resolution, for single species. Therefore, the advantages of cgLIN codes for population genomics and epidemiological questions, come at the expense of universality. Still, the dual MLSL and cgLIN code approach proposed here is in principle applicable to all bacterial species (or closely related groups thereof) for which large representative sets of genomes are available. The cgLIN code algorithms were incorporated into BIGSdb and should be readily portable to other existing cgMLST platforms such as EnteroBase. However, the use of genetic thresholds for an entire group of organisms may not always be meaningful, depending on population genetic structure. Whereas *K. pneumoniae* shows strong structuring with neat peaks and valleys of pairwise genetic distances, other species may have more fuzzy structure. In the latter cases, the approach will still be applicable, but even optimally defined thresholds may be less relevant biologically.

Conclusions

A unified nomenclature of pathogen genotypes is required to facilitate communication in the 'One Health' and 'Global Health' perspectives. *K. pneumoniae* represents a rapidly growing public health threat, and the availability of a common language to designate its emerging sublineages is therefore highly timely. The proposed unified taxonomy of *K. pneumoniae* strains will facilitate advances on the biology of its sublineages across niches, time and space, and will endow surveillance networks with the capacity to efficiently monitor and control the emergence of sublineages of high public health relevance.

Here, we propose a dual barcoding approach to bacterial strain taxonomy, which combines the complementary advantages of stability provided by the cgLIN codes, with an unstable, but human readable multilevel single linkage nomenclature rooted in the popular 7-gene MLST nomenclature. Because they are definitive, cgLIN codes can be used for the traceability of cluster fusions that will occur occasionally in the MLSL arm of the dual taxonomy (**Figure S11**). We contend the stability of cgLIN codes and their use alongside MLSL approaches provide a pragmatic solution to current attempts at developing genomic taxonomies of bacterial strains that are both stable and practical for human-to-human communication.

Material & Methods

Definition of an updated core genome MLST (scgMLSTv2) genotyping scheme

We previously defined a core genome MLST (using *strict* synteny criteria, hence name scgMLSTv1) scheme of 634 highly syntenic genes (Bialek-Davenet et al. 2014). Here, we updated the scgMLSTv1 scheme, with the following improvements. First, two loci (KP1_2104 and *aceB*=KP1_0253) were removed because they were absent or truncated in multiple strains, based on 751 high-quality assemblies available in the BIGSdb-Pasteur *Klebsiella* database on October 16th, 2017 (project id 11 at https://bigsdb.pasteur.fr/cgi-bin/bigsdb/bigsdb.pl?db=pubmlst_klebsiella_isolates&page=projects). Second, the remaining 632 loci templates were modified so that they would include the start and stop codons of the corresponding coding sequence (CDS). This was not the case for all CDSs of the scgMLSTv1 scheme, as some loci corresponded to internal portions of CDSs. These template redefinitions were done to harmonize locus definitions across the scheme. Of note, defining loci as complete CDSs also facilitates genotyping, by enabling precise identification of the extremities of novel alleles, through the search of the corresponding start and stop codons. As a result of these locus template extensions, three additional loci (yraR, rnt and KP1_1655) had to be removed because they were called in a low proportion of the above 751 genomes. The resulting 629 scgMLSTv2 genes have a summed length of 512,856 nt (9.8% of the genome of reference strain NTUH-K2044), as compared to 507,512 nt (9.7%) for the corresponding loci in scgMLSTv1.

Definition of a genomic sequence dataset of 7,060 isolates with cgMLST profiles

The *K. pneumoniae* species complex (KpSC) comprises seven phylogroups that have been given taxonomic status in the prokaryotic nomenclature: *K. pneumoniae* subsp. *pneumoniae* (Kp1, also known as *K. pneumoniae sensu stricto*), *K. quasipneumoniae* subsp. *quasipneumoniae* (Kp2), *K. variicola* subsp. *variicola* (Kp3), *K. quasipneumoniae* subsp. *similipneumoniae* (Kp4), *K. variicola* subsp. *tropica* (Kp5), '*K. quasivariicola'* (Kp6) and *K. africana* (Kp7) (Rodrigues et al. 2019). We retrieved all KpSC genomes from the GenBank assembly repository on March 15th, 2019, corresponding to 8,125 assemblies. We then chose high-quality assemblies by excluding draft genomes: (i) containing more than 1,000 contigs of size >200 nt; (ii) for which the average nucleotide identity (ANI) values (estimated using FastANI v1.1) were < 96% against every reference strain of the taxonomic diversity of the SC (Rodrigues et al., 2019; **Table S9**); (iii) of size ≤ 4.5Mb or ≥ 6.5 Mb; and (iv) with G+C% content >59%. The data of each criterion per strain are shown in **Table S1**. The three last criteria excluded possible contamination or non-KpSC genomes (**Figure S2**).

The resultant 7,388 'high-quality' draft genomes (**Table S2**) were scanned for scgMLSTv2 alleles, using the BLASTN algorithm, as implemented in the BIGSdb platform (Keith A. Jolley, Bray, and Maiden 2018; K. A. Jolley and Maiden 2010), with 90% identity, 90% length coverage, word size 30, with type alleles only (as defined below). After this step, 235 profiles were excluded because they had more than 30 missing alleles.

The resulting dataset comprised 36 taxonomic references of Kp1-Kp7 (Rodrigues et al. 2019) that, together with eight additional genomes of phylogroup Kp7, were considered as a reference dataset of the KpSC taxa ('*K. quasivariicola'* reference strain KPN1705, SB6096, was excluded because it had more than 30 missing alleles). Besides these 44 reference genomes, 7,154 GenBank genomes were retained, resulting in a total dataset of 7,198 genomes (**Table S1; Table S2**). For some analyses, 138 genomes were set aside, defined as 'hybrids' between phylogroups (see below), resulting in a 7,060-genome dataset (**Figure S2**).

We estimated within-outbreak variation using previously published outbreak sets (**Table S6, Table S7**).

Recording sequence variation at the cgMLST gene loci

Allelic variation at scgMLSTv2 loci was determined with the following strategy. First the sequence of strain NTUH-K2044 was used as the reference genome, with all its alleles defined as allele 1. Then, BLASTN searches (70% identity, 90% length coverage) were carried out using allele 1 as query against the genomic sequences of reference genomes 18A069, 342, 01A065, 07A044, CDC4241-71 and 08A119, representing major lineages (phylogroups Kp2 to Kp6, including two genomes of Kp3 and excluding Kp7, which was not discovered yet) of the KpSC (Blin et al. 2017). Only sequences with a complete CDS (start and stop, no internal frameshift) and within a plus/minus 5% range of the reference size were accepted. Alleles defined from these reference genomes and from NTUH-K2044 were then defined as type alleles.

New alleles were identified by BLASTN searches using a 90% identity threshold, 90% length coverage and a word size of 30 and the above defined type alleles. The use of type alleles avoided expanding the sequence space of alleles in an uncontrolled way, at the cost of losing a few highly divergent alleles, which may have replaced original (vertically inherited) alleles by horizontal gene transfer (HGT) and homologous recombination. As for type alleles, novel alleles were accepted only if they (i) corresponded to a complete CDS (start and stop codons with no internal frameshift mutations) and (ii) were within a 5% (plus/minus) of the size of the type allele size. Novel allele sequences were also excluded if they came from assemblies with more than 500 contigs of size > 200 nt, as these may correspond to low quality assemblies and that might contain artifactual alleles. Genome assemblies based on 454 sequencing technology, which are prone to frameshifts, were also excluded for novel allele definitions. No genome assemblies based on IonTorrent sequencing technology were found.

In order to speed the scanning process, we used the fast scan option (-e -f) of the BIGSdb autotag.pl script (https://bigsdb.readthedocs.io/en/latest/offline_tools.html). This option limits the BLASTN search to a few exemplar alleles, which are used as query to find the genomic region corresponding to the locus. In a second step, a direct database lookup of the region was performed to identify the exact allele.

Definition of MLST sequence types (ST) and core genome MLST sequence types (cgST)

Classical 7-gene MLST loci have been defined previously (Diancourt et al. 2005) as internal portions of the seven protein-coding genes *gapA*, *infB*, *mdh*, *pgi*, *phoE*, *rpoB* and *tonB*. Novel alleles were defined in the Institut Pasteur *Klebsiella* MLST and whole-genome MLST database https://bigsdb.pasteur.fr/klebsiella/. In 7-locus MLST, the combination of the seven allelic numbers determines the isolate profile, and each unique profile is attributed a sequence type (ST) number. Incomplete MLST profiles with one (or more) missing gene(s) are recorded in the isolates database but in these cases, no ST number can be attributed and the profiles are therefore not defined in the sequence definition database. The 7-locus MLST genes were not included in the scgMLSTv2 scheme.

Similar to ST identifiers used for unique 7-gene MLST allelic combinations, each distinct cgMLST profile can be assigned a unique identifier; however, when using draft genomes, cgMLST data can be partly incomplete due to *de novo* assembly shortcomings or missing loci. cgSTs were therefore defined only for cgMLST profiles with no more than 30 uncalled alleles out of the 629 cgMLSTv2 loci. In addition, we have used the --match_missing option of the define_profiles.pl script, which allows missing loci to be treated as specific alleles rather than 'any' alleles. While this retains more information (because it differentiates profiles that differ only by missing data at different loci), it can result in some isolates genomes corresponding potentially to more than a single cgST; their equality can nevertheless be deduced by the last MLSL level, ‘mismatch 0’, as these will be grouped into the same clusters at level 0; this is because the clustering ignores loci with missing data in any of the profiles of a pair when calculating the pairwise distance. For example, cgST1 = 0-N-1-1; cgST2 = 0-2-N-1; an isolate with profile 0-2-1-1 would result in cgST3 = 0-2-1-1 being created, and this genome would equate to both previous cgSTs and would be labeled as cgST1; cgST2; cgST3.

Phylogenetic analyses, recombination tests and screens for virulence and resistance genes

JolyTree v2.0 (Criscuolo 2019; 2020) was used to reconstruct a phylogenetic tree of the KpSC. For this, first a single linkage clustering was performed to cluster cgSTs into partitions. This clustering was applied on the pairwise distances between allelic profiles, defined as the number of loci with different alleles, normalized by the number of loci with alleles called in both profiles. A threshold of 8 mismatches was defined, resulting in 2,417 clusters. One genome from each of these 2,417 clusters was used as an exemplar for phylogenetic analysis (**Figure 1**).

A core genome multiple sequence alignment (cg-MSA) of 7,060 cgMLST profiles free of evidence for inter-phylogroup 'hybridization' (see below) was constructed. The gene sequences were retrieved based on allele number in the sequence definition database, individual gene sequences were aligned with MAFFT v7.467 (missing alleles were converted into gaps), and the multiple sequence alignments were concatenated. IQ-TREE v2.0.6 was used to infer a phylogenetic tree with the GTR+G model (**Figure 2**).

Locus-by-locus recombination analyses were computed with the PHI test (Bruen, Philippe, and Bryant 2006) using PhiPack v1.0.

Kleborate v2.0.4 (Lam et al. 2021) was employed to identify acquired antimicrobial resistance and virulence genes in genomic sequences, based on CARD v3.0.8 database, with identity >80% and coverage >90%. Virulence score (ranges from 0 to 5) and antimicrobial resistance score (ranges from 0 to 3) were also derived from Kleborate. The virulence score is assigned according to the presence of yersiniabactin (*ybt*), colibactin (*clb*) and aerobactin (*iuc*), as follows: 0 = none present, 1 = yersiniabactin only, 2 = yersiniabactin and colibactin (or colibactin only), 3 = aerobactin (without yersiniabactin or colibactin), 4 = aerobactin and yersiniabactin (without colibactin), and 5 = all three present. Resistance scores are calculated as follows: 0 = no ESBL (Extended-Spectrum Beta-Lactamases), no carbapenemase, 1 = ESBL without carbapenemase, 2 = carbapenemase without colistin resistance, 3 = carbapenemase with colistin resistance.

Detection of hybrid genomes

Horizontal gene transfer of large portions of the genome can occur among isolates belonging to distinct KpSC phylogroups (Holt et al. 2015). Additionally, MLST or scgMLST alleles may have been transferred horizontally from non-KpSC members, for example *E. coli*. For the purpose of phylogeny-based classification, putative hybrid genomes were excluded. To define genomes that result from large inter-phylogroup recombination events, the gene-by-gene approach was used to define an original strategy, outlined briefly here and more thoroughly in the supplementary appendix (Detection of hybrids): for each locus, each allele was unambiguously labelled by one of the seven KpSC phylogroup of origin, if possible; next, for each profile, a phylogroup homogeneity index (*i.e.*, proportion of alleles labelled by the predominant phylogroup) was derived. The distributions of the phylogroup homogeneity indices allowed determining hybrid genomes (**Figure S12**). Exclusion of such hybrid genomes resulted in a genomic dataset of 7,060 isolates deemed as having a majority of alleles inherited from within a single phylogroup. Of the 44 reference genomes, one (SB1124, of phylogroup Kp2) was defined as having a hybrid origin: 414 alleles were attributed to Kp2, whereas 150 alleles originated from non-KpSC species; as a result, 73.4% of SB1124 alleles were part of the majority phylogroup, which was below the defined threshold of 78%. The quantification of recombination breakpoints was performed based on the position of cgMLST loci on the NTUH-K2044 reference genome (NC_012731), counting the number of recombination breakpoints in each successive 500 kb fragment along the reference genome. Note that hybrids had typical assembly sizes (**Table S1**), whereas our simulations of contaminated sequence read sets between phylogroups resulted in significantly larger assemblies (not shown; available upon request).

Identification of genetic discontinuities in the KpSC population structure

The tool MSTclust v0.21b (https://gitlab.pasteur.fr/GIPhy/MSTclust) was used to perform the single linkage clustering of cgMLST profiles from their pairwise allelic mismatch dissimilarities, as well as to assess the efficiency of the resulting profile partitioning (for details, see supplementary appendix: Minimum Spanning tree-based clustering of cgMLST profiles). Briefly, for each threshold *t* (= 0 to 629 allelic mismatches), the clustering consistency was assessed using the silhouette metrics S_t (Rousseeuw 1987), whereas its robustness to profile subsampling biases was assessed using a dedicated metrics W_t based on the adjusted Wallace coefficients (Wallace 1983; Severiano et al. 2011). Both consistency (S_t) and stability (W_t) coefficients converge to 1 when the threshold *t* leads to a clustering that is consistent with the 'natural' grouping and is robust to subsampling biases, respectively.

The adjusted Rand index R_t (Carrico et al. 2006; Hubert and Arabie 1985) was used to assess the global concordance between single linkage clustering partitions and those induced by classifications into 7-gene MLST sequence types, subspecies and species.

Diversity and phylogenetic compatibility indices

Simpson's diversity index was computed using the www.comparingpartitions.info website (Carrico et al. 2006). The clade compatibility index of STs or other groups was calculated using the ETE Python library (http://etetoolkit.org/docs/latest/tutorial/tutorial_trees.html#checking-the-monophyly-of-attributes-within-a-tree), in order to define whether their constitutive genomes formed a monophyletic, paraphyletic or polyphyletic group within the recombination-purged sequence-based phylogeny of the core genome. We estimated clade compatibility as the proportion of non-singleton STs, sublineages or clonal groups that were monophyletic.

Classification of cgMLST profiles into clonal groups and sublineages

The classification scheme functionality was implemented within BIGSdb v1.14.0 and relies on single linkage clustering. Briefly, cgSTs were defined in the sequence definitions ('seqdef') database as distinct profiles with fewer than 30 missing alleles over the scgMLST scheme, and their pairwise cgMLST distance was computed as the number of distinct alleles. To account for missing data, a relative threshold was used for clustering: the number of allelic mismatches was multiplied by the proportion of loci for which an allele was called in both strains. Hence, in order to be grouped, the number of matching alleles must exceed: (the number of loci called in both strains × (total loci - defined threshold)) / total loci. cgSTs and their corresponding sublineage (SL), clonal group (CG) and other levels partition identifiers, are stored in the seqdef database and are publicly available. Here, classification schemes were defined in the *Klebsiella* seqdef database on top of the scgMLSTv2 scheme, and host single linkage clustering group identifiers at the 10 defined cgMLST allelic mismatch thresholds (see Results). For classification groups defined using 43 and 190 allelic mismatch thresholds, scheme fields were defined and populated with the identifiers defined by inheritance from 7-gene MLST ST identifiers (see supplementary appendix: Nomenclature inheritance algorithm).

Adaptation of the LIN code approach to cgMLST: defining cgLIN codes

Vinatzer and colleagues proposed an original nomenclature method in which each genome is attributed a Life Identification Number code (LIN code), based on genetic similarity with the closest previously encoded member of the nomenclature (Marakeby et al. 2014; Weisberg et al. 2015;

Vinatzer et al. 2016; Vinatzer, Tian, and Heath 2017; Tian et al. 2020). In this proposal, the similarity between genomes was based on ANI (Average Nucleotide Identity; (Konstantinidis and Tiedje 2005; Goris et al. 2007)), with a set of 24 thresholds corresponding to ANI percentages of 60, 70, 75, 80, 85, 90, 95, 98, 98.5, 99, 99.25, 99.5, 99.75, 99.9, 99.925, 99.95, 99.975, 99.99, 99.999 and 99.9999. Here, the method was adapted by replacing the ANI metric by the similarity between cgMLST profiles, defined as the proportion of loci with identical alleles normalized by the number of loci with alleles called in both profiles. These codes, which we refer to as cgLIN codes, are composed of a set of *p* positions, each corresponding to a pairwise genome similarity threshold s_p. These similarity thresholds are sorted in ascending order (*i.e.*, $s_p < s_{p+1}$), the first positions of the code (on the left side) thus corresponding to low levels of similarity. Following the initial proposal, the codes are assigned as follows (**Figure S13**): (step 1) the code is initialized with the first strain being assigned the value "0" at all positions; (step 2) the encoding rule for a new genome *i* is based on the closest genome *j* already encoded as follows, from the similarity $s_{ij} \in]\, s_{p-1} , s_p \,]$:

i) identical to code *j* up to and including position *p* – 1;

ii) for the position *p*: maximum value observed at this position (among the subset of codes sharing the same prefix at the position *p* – 1) incremented by 1;

iii) "0" to all downstream positions, from *p* + 1 included.

For each genome to be encoded, step 2 is repeated.

A set of 10 cgMLST thresholds were defined as follows: first, four thresholds were chosen above the similarity values peak observed between *Klebsiella* species (s_p = 1 – 610 / 629 = 0.03), subspecies (s_p = 1 – 585 / 629 = 0.07), main sublineages (s_p = 1 – 190 / 629 = 0.70) and clonal groups (s_p =1 – 43 / 629 = 0.93). Second, we included six thresholds deemed useful for epidemiological studies, corresponding to 10, 7, 4, 2, 1 and 0 allelic mismatches.

This encoding system conveys phylogenetic information, as two genomes with identical prefixes in their respective cgLIN codes can be understood as being similar, to an extent determined by the length of their common prefix. Isolates having cgMLST profiles with 100% identity (no mismatch at loci called in both genomes) will have exactly the same cgLIN code. For example, cgLIN codes 0_0_22_12_0_1_0_0_0_0 and 4_0_3_0_0_0_0_0_0_0 would denote two strains belonging to distinct species (as they differ by their first number in the code). cgLIN codes 0_0_105_6_0_0_75_1_1_0 and 0_0_105_6_0_0_75_1_0_0 correspond to strains from Kp1 (prefix 0_0) that differ by only 2 loci; they are identical up to the second bin, corresponding to 2 locus mismatches (**Figure S13**); note that 0 and

1 mismatches are both included in the last bin: genomes have an identical identifier when having 0 difference, and a different identifier when having 1 mismatch (**Figure S14**).

The impact of genome input order on the number of cgLIN code partitions at a given threshold was defined using the 7,060 high-quality, non-hybrid cgMLST profiles, which were encoded 500 times with random input orders (see details in the supplementary appendix: Impact of strains input order on LIN codes, and use of Prim's algorithm).

The scripts for cgLIN code database creation were made available via GitLab BEBP (https://gitlab.pasteur.fr/BEBP/LINcoding).

Acknowledgements

This work builds partly on the classical 7-gene MLST database, which has been curated by Virginie Passet, Radek Izdebski, Carla Rodrigues and Federica Palma. We thank Adrien Le Meur for help with the genome dataset constitution and initial analyses of intra-outbreak variation.

Funding

MH was supported financially by the PhD grant "Codes4strains" from the European Joint Programme One Health, which has received funding from the European Union's Horizon 2020 Research and Innovation Programme under Grant Agreement No. 773830. This work was supported financially by the French Government's Investissement d'Avenir program Laboratoire d'Excellence "Integrative Biology of Emerging Infectious Diseases" (ANR-10-LABX-62-IBEID) and by an award from the Bill and Melinda Gates Foundation (INV-025280). BIGSdb development is funded by a Wellcome Trust Biomedical Resource grant (218205/Z/19/Z). This work used the computational and storage services provided by the IT department at Institut Pasteur.

Authors license statement

This research was funded, in whole or in part, by Institut Pasteur and by European Union's Horizon 2020 research and innovation programme. For the purpose of open access, the authors have applied a CC-BY public copyright license to any Author Manuscript version arising from this submission.

Declaration of interest statement: The authors declare no conflict of interest.

Ethical approval statement: Not relevant.

Author contributions

S.B. designed and coordinated the study. M.H. performed the genomic analyses, and cgLIN code developments and implementations. J.G. designed the novel version of the cgMLST scheme. A.C. developed the MSTclust tool (and associated metrics), and supervised cgLIN developments and phylogenetic analyses. K.A.J. and M.C.J.M. designed and developed the BIGSdb platform, with help from S. Bridel for the integration of cgLIN code functionality. S.B. and M.H. wrote the initial version of the manuscript, with input from A.C. All authors provided input to the manuscript and reviewed the final version.

Figure legends

Figure 1. **Genome-based phylogenetic tree of the *K. pneumoniae* species complex.**

The whole-genome distance-based tree was inferred using JolyTree. JolyTree uses *mash* to decompose each genome into a sketch of k-mers and to quickly estimate the p-distance between each pair of genomes; after transforming every p-distance into a pairwise evolutionary distance, a phylogenetic tree is inferred using FastME. The seven phylogroups are indicated. Red dots correspond to strains defined as inter-phylogroup hybrids. Scale bar, 0.01 nucleotide substitutions per site.

Figure 2. **Phylogenetic structure within phylogroup Kp1 (*K. pneumoniae sensu stricto*).**

The circular tree was obtained using IQ-TREE based on the concatenation of the genes of the scgMLSTv2 scheme; 1,600 isolates are included (see Methods). Labels on the external first circle represent 7-gene MLST ST identifiers (each alternation corresponds to a different ST and only ST with more than 20 strains are labelled). The second and third circles (light green and blue, respectively) show the alternation of clonal groups (CG) and sublineages (SL), respectively, labelling only groups with more than 20 isolates. Full correspondence between ST, SL and CG identifiers is given in the supplementary appendix.

Figure 3. **Distribution of pairwise cgMLST distances, clustering properties and phylogenetic congruence**.

Values are plotted for the 7,060 genomes dataset. Threshold values (t) are shown on the X-axis, corresponding to allelic profile mismatch values up to 629 (or 100%). Grey histograms: distribution of pairwise allelic mismatches. The circles correspond to the different modes of distribution. The curves represent the consistency (silhouette) and stability coefficients S_t (blue) and W_t (green), respectively, obtained with each threshold t; the corresponding scale is on the left Y-axis. The dotted vertical red lines at t = 43/629, 190/629, 585/629 and 610/629 represent the thresholds up to which pairs of genomes belong to the same clonal groups, sublineages, phylogroups and species, respectively.

Figure 4. Concordance of sublineage, clonal group and 7-gene MLST classifications.

Alluvial diagram obtained using RAWGraphs (Mauri *et al.* 2017: doi.org/10.1145/3125571.3125585) showing the correspondence between sequence types (ST; 7 genes identity), clonal groups (CG; 43 allelic mismatches threshold) and sublineages (SL; 190 allelic mismatches threshold). Colors are arbitrarily attributed by the software for readability.

Figure 5. Phylogenetic relationships are reflected in cgLIN code prefixes.

Left: the prefix tree generated from cgLIN codes; Right: phylogenetic relationships derived using IQ-TREE from the cgMLST gene sequences from the reference strains. The cgLIN codes are also shown. The values indicated on top of the prefix tree correspond to the cgMLST similarity percentage of the corresponding cgLIN code bin.

Figure 6. cgLIN code prefixes, and virulence and antimicrobial resistance scores of some sublineages and their clonal groups.

Left (green) panel: LIN prefixes of selected sublineages (SL) and clonal groups (CG). Right: heatmaps of virulence and resistance scores of clonal groups, and the number of genomes in each group. For each genome, the virulence score derived from Kleborate has a value from 0 to 5; the value in the cells corresponds to the percentage of strains in the group with that virulence score (similar to a heat map). The principle is the same for the resistance score, but it varies from 0 to 3.

Tables

Table 1. Genome dataset phylogroup breakdown, quality assessment and diversity.

References

Achtman, Mark, John Wain, François-Xavier Weill, Satheesh Nair, Zhemin Zhou, Vartul Sangal, Mary G. Krauland, et al. 2012. 'Multilocus Sequence Typing as a Replacement for Serotyping in Salmonella Enterica'. *PLoS Pathog* 8 (6): e1002776. https://doi.org/10.1371/journal.ppat.1002776.

Barker, Dillon OR, João A. Carriço, Peter Kruczkiewicz, Federica Palma, Mirko Rossi, and Eduardo N. Taboada. 2018. 'Rapid Identification of Stable Clusters in Bacterial Populations Using the Adjusted Wallace Coefficient'. *BioRxiv*, April, 299347. https://doi.org/10.1101/299347.

Belkum, A. van, P. T. Tassios, L. Dijkshoorn, S. Haeggman, B. Cookson, N. K. Fry, V. Fussing, et al. 2007. 'Guidelines for the Validation and Application of Typing Methods for Use in Bacterial Epidemiology'. *Clin Microbiol Infect* 13 Suppl 3 (October): 1–46.

Bialek-Davenet, S., A. Criscuolo, F. Ailloud, V. Passet, L. Jones, A. S. Delannoy-Vieillard, B. Garin, et al. 2014. 'Genomic Definition of Hypervirulent and Multidrug-Resistant Klebsiella Pneumoniae Clonal Groups'. *Emerg Infect Dis* 20 (11): 1812–20. https://doi.org/10.3201/eid2011.140206.

Blin, C., V. Passet, M. Touchon, E. P. C. Rocha, and S. Brisse. 2017. 'Metabolic Diversity of the Emerging Pathogenic Lineages of Klebsiella Pneumoniae'. *Environ Microbiol* 19 (5): 1881–98. https://doi.org/10.1111/1462-2920.13689.

Bowers, Jolene R., Brandon Kitchel, Elizabeth M. Driebe, Duncan R. MacCannell, Chandler Roe, Darrin Lemmer, Tom de Man, et al. 2015. 'Genomic Analysis of the Emergence and Rapid Global Dissemination of the Clonal Group 258 Klebsiella Pneumoniae Pandemic'. *PloS One* 10 (7): e0133727. https://doi.org/10.1371/journal.pone.0133727.

Brisse, S., F. Grimont, and P.A.D. Grimont. 2006. 'The Genus Klebsiella'. In *The Prokaryotes A Handbook on the Biology of Bacteria*, 3rd edition, 159–96. New York: Springer.

Brisse, S., and J. Verhoef. 2001. 'Phylogenetic Diversity of Klebsiella Pneumoniae and Klebsiella Oxytoca Clinical Isolates Revealed by Randomly Amplified Polymorphic DNA, GyrA and ParC Genes Sequencing and Automated Ribotyping'. *Int J Syst Evol Microbiol* 51 (Pt 3): 915–24.

Bruen, Trevor C., Hervé Philippe, and David Bryant. 2006. 'A Simple and Robust Statistical Test for Detecting the Presence of Recombination'. *Genetics* 172 (4): 2665–81. https://doi.org/10.1534/genetics.105.048975.

Carrico, J. A., C. Silva-Costa, J. Melo-Cristino, F. R. Pinto, H. de Lencastre, J. S. Almeida, and M. Ramirez. 2006. 'Illustration of a Common Framework for Relating Multiple Typing Methods by Application to Macrolide-Resistant Streptococcus Pyogenes'. *J Clin Microbiol* 44 (7): 2524–32. https://doi.org/10.1128/JCM.02536-05.

Chen, Liang, Barun Mathema, Johann D. D. Pitout, Frank R. DeLeo, and Barry N. Kreiswirth. 2014. 'Epidemic Klebsiella Pneumoniae ST258 Is a Hybrid Strain'. *MBio* 5 (3): e01355-01314. https://doi.org/10.1128/mBio.01355-14.

Cowan, S. T. 1965. 'PRINCIPLES AND PRACTICE OF BACTERIAL TAXONOMY--A FORWARD LOOK'. *Journal of General Microbiology* 39 (April): 143–53. https://doi.org/10.1099/00221287-39-1-143.

Criscuolo, Alexis. 2019. 'A Fast Alignment-Free Bioinformatics Procedure to Infer Accurate Distance-Based Phylogenetic Trees from Genome Assemblies'. *Research Ideas and Outcomes* 5 (June): e36178. https://doi.org/10.3897/rio.5.e36178.

———. 2020. 'On the Transformation of MinHash-Based Uncorrected Distances into Proper Evolutionary Distances for Phylogenetic Inference'. *F1000Research* 9 (November): 1309. https://doi.org/10.12688/f1000research.26930.1.

Dallman, Timothy, Philip Ashton, Ulf Schafer, Aleksey Jironkin, Anais Painset, Sharif Shaaban, Hassan Hartman, et al. 2018. 'SnapperDB: A Database Solution for Routine Sequencing Analysis of Bacterial Isolates'. *Bioinformatics (Oxford, England)* 34 (17): 3028–29. https://doi.org/10.1093/bioinformatics/bty212.

Diancourt, L., V. Passet, J. Verhoef, P. A. Grimont, and S. Brisse. 2005. 'Multilocus Sequence Typing of Klebsiella Pneumoniae Nosocomial Isolates'. *J Clin Microbiol* 43 (8): 4178–82.

Feil, E. J. 2004. 'Small Change: Keeping Pace with Microevolution'. *Nat. Rev. Microbiol.* 2 (6): 483–95.

Fevre, C., V. Passet, F. X. Weill, P. A. Grimont, and S. Brisse. 2005. 'Variants of the Klebsiella Pneumoniae OKP Chromosomal Beta-Lactamase Are Divided into Two Main Groups, OKP-A and OKP-B'. *Antimicrob Agents Chemother* 49 (12): 5149–52.

Goris, J., K. T. Konstantinidis, J. A. Klappenbach, T. Coenye, P. Vandamme, and J. M. Tiedje. 2007. 'DNA-DNA Hybridization Values and Their Relationship to Whole-Genome Sequence Similarities'. *Int J Syst Evol Microbiol* 57 (Pt 1): 81–91.

Hacker, J., and J. B. Kaper. 2000. 'Pathogenicity Islands and the Evolution of Microbes'. *Annu Rev Microbiol* 54: 641–79.

Holt, K. E., H. Wertheim, R. N. Zadoks, S. Baker, C. A. Whitehouse, D. Dance, A. Jenney, et al. 2015. 'Genomic Analysis of Diversity, Population Structure, Virulence, and Antimicrobial Resistance in Klebsiella Pneumoniae, an Urgent Threat to Public Health'. *Proc Natl Acad Sci U S A* 112 (27): E3574-81. https://doi.org/10.1073/pnas.1501049112.

Hubert, Lawrence, and Phipps Arabie. 1985. 'Comparing Partitions'. *Journal of Classification* 2 (1): 193–218. https://doi.org/10.1007/BF01908075.

Jolley, K. A., and M. C. Maiden. 2010. 'BIGSdb: Scalable Analysis of Bacterial Genome Variation at the Population Level'. *BMC Bioinformatics* 11: 595. https://doi.org/10.1186/1471-2105-11-595.

Jolley, Keith A., James E. Bray, and Martin C. J. Maiden. 2018. 'Open-Access Bacterial Population Genomics: BIGSdb Software, the PubMLST.Org Website and Their Applications'. *Wellcome Open Research* 3: 124. https://doi.org/10.12688/wellcomeopenres.14826.1.

Konstantinidis, Konstantinos T., and James M. Tiedje. 2005. 'Genomic Insights That Advance the Species Definition for Prokaryotes'. *Proceedings of the National Academy of Sciences of the United States of America* 102 (7): 2567–72. https://doi.org/10.1073/pnas.0409727102.

Lam, Margaret M. C., Ryan R. Wick, Stephen C. Watts, Louise T. Cerdeira, Kelly L. Wyres, and Kathryn E. Holt. 2021. 'A Genomic Surveillance Framework and Genotyping Tool for Klebsiella Pneumoniae and Its Related Species Complex'. *Nature Communications* 12 (1): 4188. https://doi.org/10.1038/s41467-021-24448-3.

Lam, Margaret M. C., Kelly L. Wyres, Sebastian Duchêne, Ryan R. Wick, Louise M. Judd, Yunn-Hwen Gan, Chu-Han Hoh, et al. 2018. 'Population Genomics of Hypervirulent Klebsiella Pneumoniae Clonal-Group 23 Reveals Early Emergence and Rapid Global Dissemination'. *Nature Communications* 9 (1): 2703. https://doi.org/10.1038/s41467-018-05114-7.

Lan, R., and P. R. Reeves. 2001. 'When Does a Clone Deserve a Name? A Perspective on Bacterial Species Based on Population Genetics'. *Trends Microbiol* 9: 419–24.

Long, S. Wesley, Sarah E. Linson, Matthew Ojeda Saavedra, Concepcion Cantu, James J. Davis, Thomas Brettin, and Randall J. Olsen. 2017. 'Whole-Genome Sequencing of a Human Clinical Isolate of the Novel Species Klebsiella Quasivariicola Sp. Nov'. *Genome Announcements* 5 (42). https://doi.org/10.1128/genomeA.01057-17.

Maiden, M. C., J. A. Bygraves, E. Feil, G. Morelli, J. E. Russell, R. Urwin, Q. Zhang, et al. 1998. 'Multilocus Sequence Typing: A Portable Approach to the Identification of Clones within Populations of Pathogenic Microorganisms'. *Proc. Natl. Acad. Sci. U. S. A.* 95 (6): 3140–45.

Maiden, M. C., M. J. van Rensburg, J. E. Bray, S. G. Earle, S. A. Ford, K. A. Jolley, and N. D. McCarthy. 2013. 'MLST Revisited: The Gene-by-Gene Approach to Bacterial Genomics'. *Nat Rev Microbiol* 11 (10): 728–36. https://doi.org/10.1038/nrmicro3093.

Marakeby, Haitham, Eman Badr, Hanaa Torkey, Yuhyun Song, Scotland Leman, Caroline L. Monteil, Lenwood S. Heath, and Boris A. Vinatzer. 2014. 'A System to Automatically Classify and Name Any Individual Genome-Sequenced Organism Independently of Current Biological Classification and Nomenclature'. *PloS One* 9 (2): e89142. https://doi.org/10.1371/journal.pone.0089142.

Miro, Elisenda, John W. A. Rossen, Monika A. Chlebowicz, Dag Harmsen, Sylvain Brisse, Virginie Passet, Ferran Navarro, Alex W. Friedrich, and S. García-Cobos. 2020. ‘Core/Whole Genome Multilocus Sequence Typing and Core Genome SNP-Based Typing of OXA-48-Producing Klebsiella Pneumoniae Clinical Isolates From Spain’. *Frontiers in Microbiology* 10: 2961. https://doi.org/10.3389/fmicb.2019.02961.

Moura, Alexandra, Alexis Criscuolo, Hannes Pouseele, Mylène M. Maury, Alexandre Leclercq, Cheryl Tarr, Jonas T. Björkman, et al. 2016. ‘Whole Genome-Based Population Biology and Epidemiological Surveillance of Listeria Monocytogenes’. *Nature Microbiology* 2 (October): 16185. https://doi.org/10.1038/nmicrobiol.2016.185.

Prim, R. C. 1957. ‘Shortest Connection Networks And Some Generalizations’. *Bell System Technical Journal* 36 (6): 1389–1401. https://doi.org/10.1002/j.1538-7305.1957.tb01515.x.

Rambaut, Andrew, Edward C. Holmes, Áine O’Toole, Verity Hill, John T. McCrone, Christopher Ruis, Louis du Plessis, and Oliver G. Pybus. 2020. ‘A Dynamic Nomenclature Proposal for SARS-CoV-2 Lineages to Assist Genomic Epidemiology’. *Nature Microbiology* 5 (11): 1403–7. https://doi.org/10.1038/s41564-020-0770-5.

Rodrigues, Carla, Virginie Passet, Andriniaina Rakotondrasoa, Thierno Abdoulaye Diallo, Alexis Criscuolo, and Sylvain Brisse. 2019. ‘Description of Klebsiella Africanensis Sp. Nov., Klebsiella Variicola Subsp. Tropicalensis Subsp. Nov. and Klebsiella Variicola Subsp. Variicola Subsp. Nov’. *Research in Microbiology*, February. https://doi.org/10.1016/j.resmic.2019.02.003.

Rousseeuw, Peter J. 1987. ‘Silhouettes: A Graphical Aid to the Interpretation and Validation of Cluster Analysis’. *Journal of Computational and Applied Mathematics* 20 (November): 53–65. https://doi.org/10.1016/0377-0427(87)90125-7.

Selander, R. K., and B. R. Levin. 1980. ‘Genetic Diversity and Structure in Escherichia Coli Populations’. *Science* 210 (4469): 545–47.

Severiano, Ana, Francisco R. Pinto, Mário Ramirez, and João A. Carriço. 2011. ‘Adjusted Wallace Coefficient as a Measure of Congruence between Typing Methods’. *Journal of Clinical Microbiology* 49 (11): 3997–4000. https://doi.org/10.1128/JCM.00624-11.

Sneath, P. H. A. 1992. *International Code of Nomenclature of Bacteria*. 1990 revision. Washington, D.C.: American Society for Microbiology.

Struelens, M. J., Y. De Gheldre, and A. Deplano. 1998. ‘Comparative and Library Epidemiological Typing Systems: Outbreak Investigations versus Surveillance Systems’. *Infect Control Hosp Epidemiol* 19 (8): 565–69.

Struve, Carsten, Chandler C. Roe, Marc Stegger, Steen G. Stahlhut, Dennis S. Hansen, David M. Engelthaler, Paal S. Andersen, Elizabeth M. Driebe, Paul Keim, and Karen A. Krogfelt. 2015. ‘Mapping the Evolution of Hypervirulent Klebsiella Pneumoniae’. *MBio* 6 (4): e00630. https://doi.org/10.1128/mBio.00630-15.

Tian, Long, Chengjie Huang, Reza Mazloom, Lenwood S Heath, and Boris A Vinatzer. 2020. ‘LINbase: A Web Server for Genome-Based Identification of Prokaryotes as Members of Crowdsourced Taxa’. *Nucleic Acids Research* 48 (W1): W529–37. https://doi.org/10.1093/nar/gkaa190.

Turner, K. M., and E. J. Feil. 2007. ‘The Secret Life of the Multilocus Sequence Type’. *Int J Antimicrob Agents* 29 (2): 129–35.

Vinatzer, Boris A., Long Tian, and Lenwood S. Heath. 2017. ‘A Proposal for a Portal to Make Earth’s Microbial Diversity Easily Accessible and Searchable’. *Antonie van Leeuwenhoek* 110 (10): 1271–79. https://doi.org/10.1007/s10482-017-0849-z.

Vinatzer, Boris A., Alexandra J. Weisberg, Caroline L. Monteil, Haitham A. Elmarakeby, Samuel K. Sheppard, and Lenwood S. Heath. 2016. ‘A Proposal for a Genome Similarity-Based Taxonomy for Plant-Pathogenic Bacteria That Is Sufficiently Precise to Reflect Phylogeny, Host Range, and Outbreak Affiliation Applied to Pseudomonas Syringae Sensu Lato as a Proof of Concept’. *Phytopathology®* 107 (1): 18–28. https://doi.org/10.1094/PHYTO-07-16-0252-R.

Vos, Michiel, and Xavier Didelot. 2009. ‘A Comparison of Homologous Recombination Rates in Bacteria and Archaea’. *The ISME Journal* 3 (2): 199–208. https://doi.org/10.1038/ismej.2008.93.

Wallace, David L. 1983. ‘A Method for Comparing Two Hierarchical Clusterings: Comment’. *Journal of the American Statistical Association* 78 (383): 569–76. https://doi.org/10.2307/2288118.

Weisberg, Alexandra J., Haitham A. Elmarakeby, Lenwood S. Heath, and Boris A. Vinatzer. 2015. ‘Similarity-Based Codes Sequentially Assigned to Ebolavirus Genomes Are Informative of Species Membership, Associated Outbreaks, and Transmission Chains’. *Open Forum Infectious Diseases* 2 (ofv024). https://doi.org/10.1093/ofid/ofv024.

Wyres, Kelly L., Claire Gorrie, David J. Edwards, Heiman F. L. Wertheim, Li Yang Hsu, Nguyen Van Kinh, Ruth Zadoks, Stephen Baker, and Kathryn E. Holt. 2015. ‘Extensive Capsule Locus Variation and Large-Scale Genomic Recombination within the Klebsiella Pneumoniae Clonal Group 258’. *Genome Biology and Evolution* 7 (5): 1267–79. https://doi.org/10.1093/gbe/evv062.

Wyres, Kelly L., Margaret M. C. Lam, and Kathryn E. Holt. 2020. ‘Population Genomics of Klebsiella Pneumoniae’. *Nature Reviews. Microbiology* 18 (6): 344–59. https://doi.org/10.1038/s41579-019-0315-1.

Wyres, Kelly L., To N. T. Nguyen, Margaret M. C. Lam, Louise M. Judd, Nguyen van Vinh Chau, David A. B. Dance, Margaret Ip, et al. 2020. ‘Genomic Surveillance for Hypervirulence and Multi-Drug Resistance in Invasive Klebsiella Pneumoniae from South and Southeast Asia’. *Genome Medicine* 12 (1): 11. https://doi.org/10.1186/s13073-019-0706-y.

Zhou, Zhemin, Jane Charlesworth, and Mark Achtman. 2021. ‘HierCC: A Multi-Level Clustering Scheme for Population Assignments Based on Core Genome MLST’. *Bioinformatics (Oxford, England)*, April, btab234. https://doi.org/10.1093/bioinformatics/btab234.

Figure 1

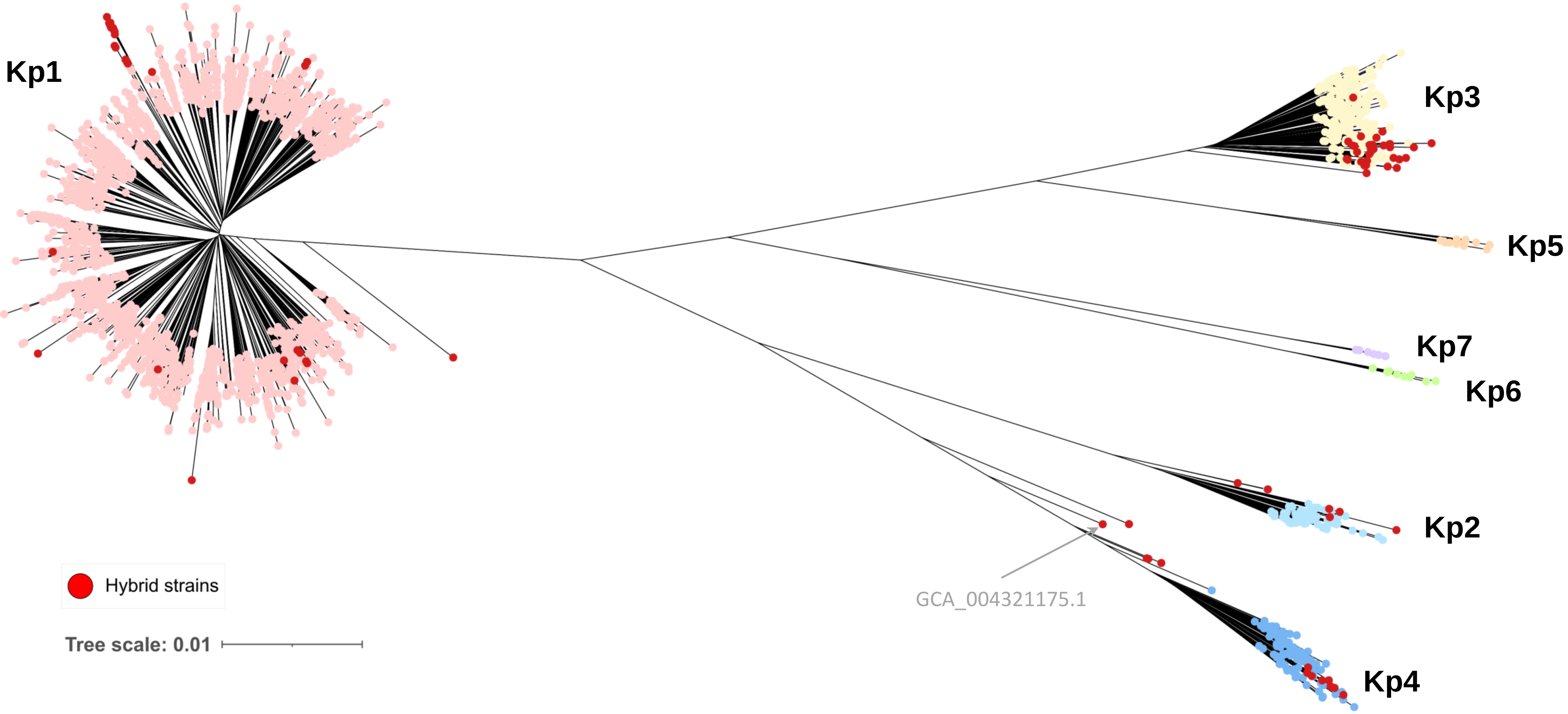
Kp1
Kp3
Kp5
Kp7
Kp6
Kp2
Kp4
GCA_004321175.1
● Hybrid strains
Tree scale: 0.01

Figure 2

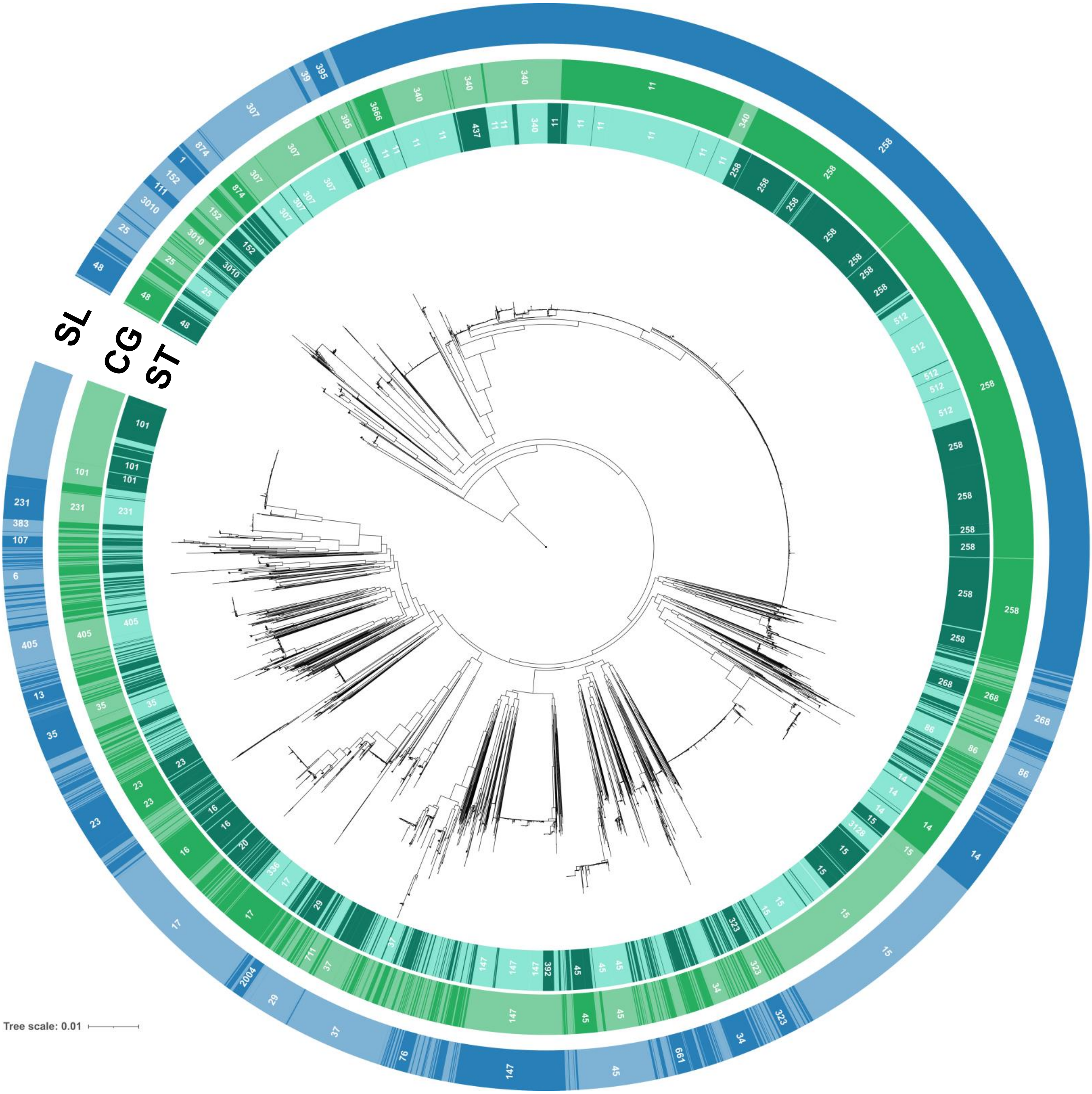
SL
CG
ST
Tree scale: 0.01
395
39
307
874
1
152
111
3010
25
48
258
268
86
14
15
323
34
661
45
147
76
37
29
2004
17
23
35
13
405
6
107
383
231
340
11
3666
395
307
874
152
3010
25
48
258
268
86
14
15
323
34
45
147
37
711
17
16
23
35
405
231
101
437
11
340
11
395
307
152
3010
25
48
258
512
268
86
14
15
3128
15
323
45
392
147
37
29
17
336
20
16
23
35
405
231
101

Figure 3

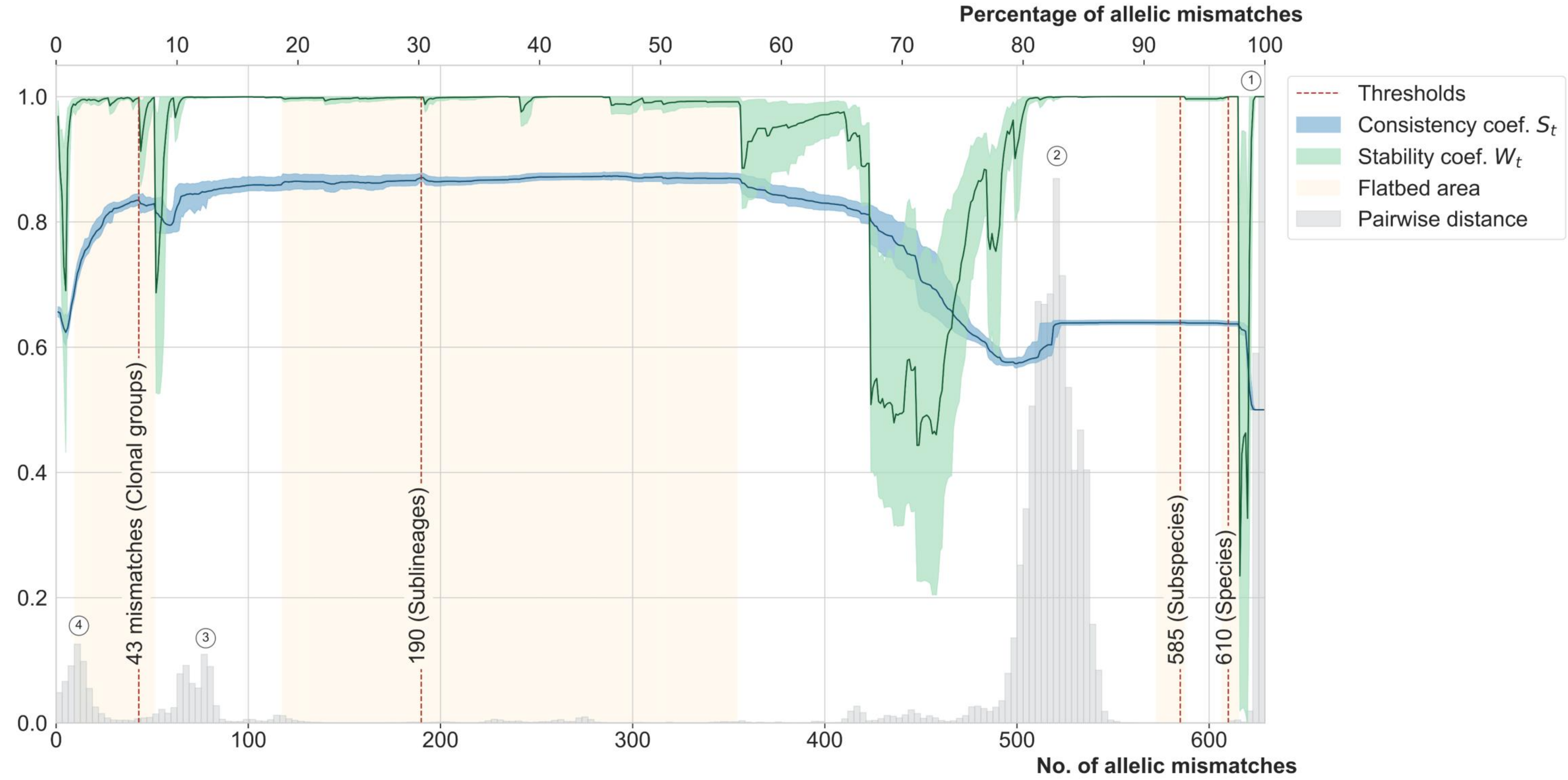
Percentage of allelic mismatches
0
10
20
30
40
50
60
70
80
90
100
1.0
0.8
0.6
0.4
0.2
0.0
0
100
200
300
400
500
600
No. of allelic mismatches
43 mismatches (Clonal groups)
190 (Sublineages)
585 (Subspecies)
610 (Species)
1
2
3
4
Thresholds
Consistency coef. S_t
Stability coef. W_t
Flatbed area
Pairwise distance

Figure 4

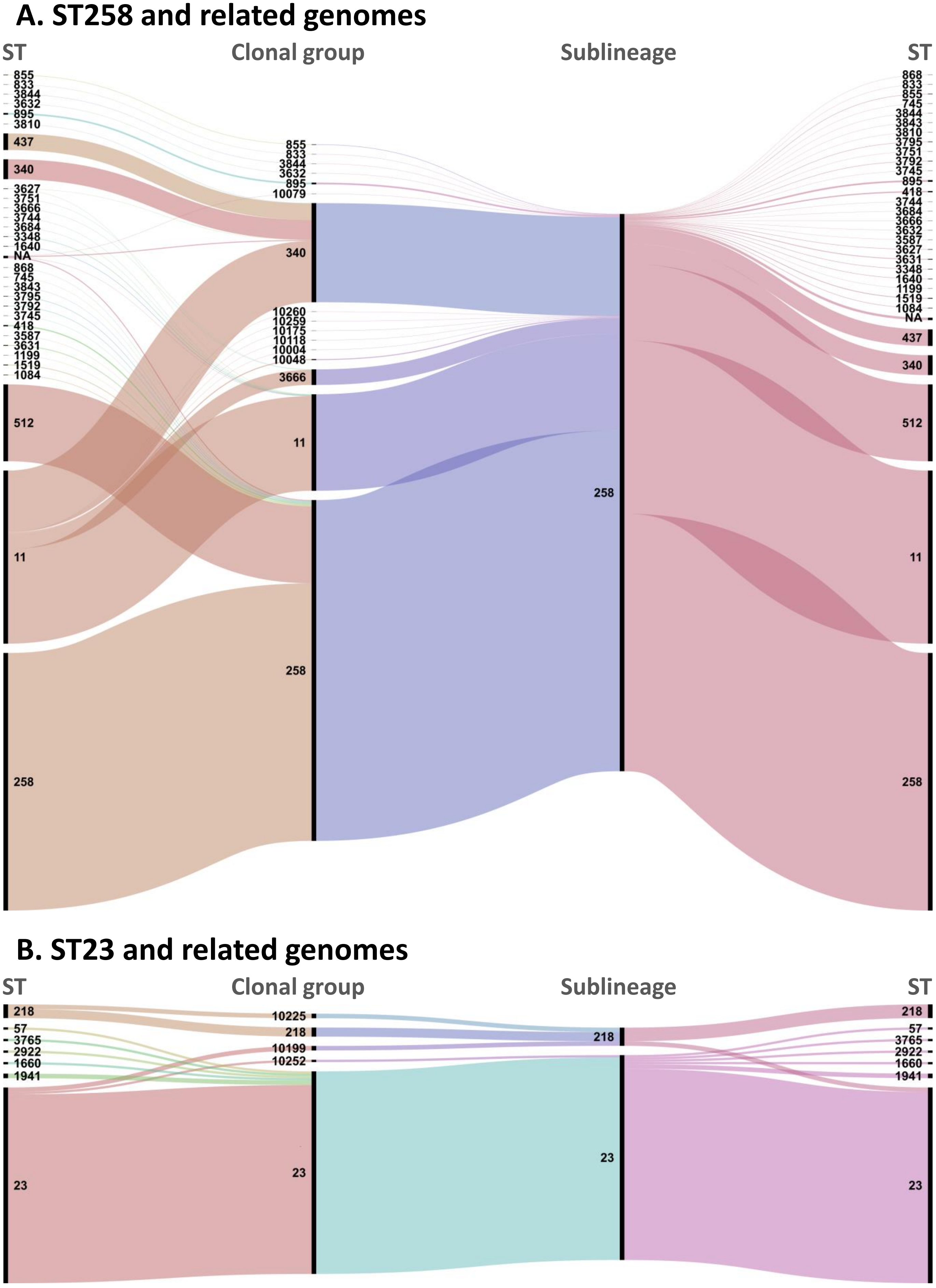

A. ST258 and related genomes

B. ST23 and related genomes

Figure 5

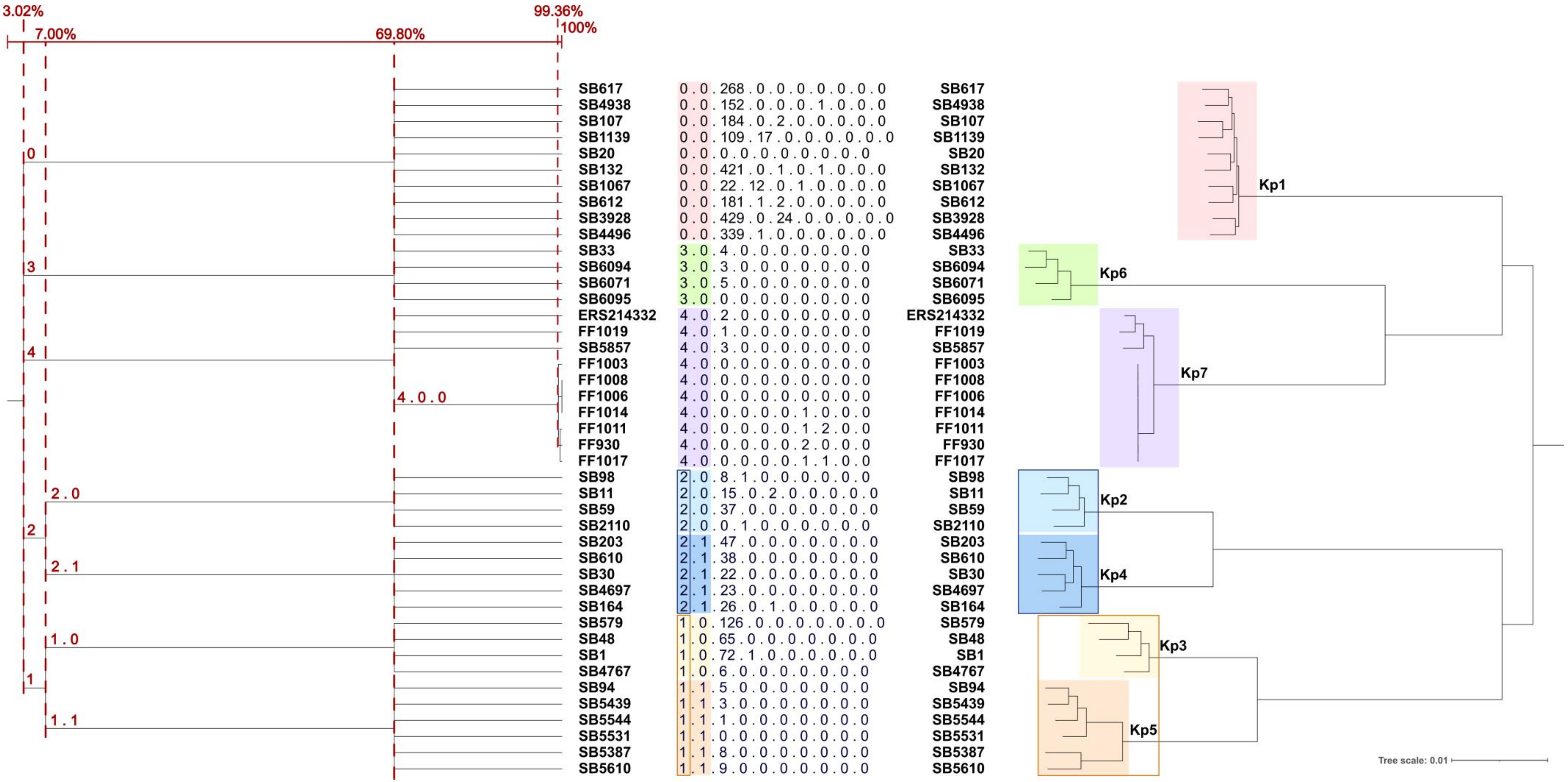

3.02%
7.00%
69.80%
99.36%
100%
0
3
4
4.0.0
2.0
2
2.1
1.0
1
1.1
SB617 0.0.268.0.0.0.0.0.0.0 SB617
SB4938 0.0.152.0.0.0.1.0.0.0 SB4938
SB107 0.0.184.0.2.0.0.0.0.0 SB107
SB1139 0.0.109.17.0.0.0.0.0.0 SB1139
SB20 0.0.0.0.0.0.0.0.0.0 SB20
SB132 0.0.421.0.1.0.1.0.0.0 SB132
SB1067 0.0.22.12.0.1.0.0.0.0 SB1067
SB612 0.0.181.1.2.0.0.0.0.0 SB612
SB3928 0.0.429.0.24.0.0.0.0.0 SB3928
SB4496 0.0.339.1.0.0.0.0.0.0 SB4496
SB33 3.0.4.0.0.0.0.0.0.0 SB33
SB6094 3.0.3.0.0.0.0.0.0.0 SB6094
SB6071 3.0.5.0.0.0.0.0.0.0 SB6071
SB6095 3.0.0.0.0.0.0.0.0.0 SB6095
ERS214332 4.0.2.0.0.0.0.0.0.0 ERS214332
FF1019 4.0.1.0.0.0.0.0.0.0 FF1019
SB5857 4.0.3.0.0.0.0.0.0.0 SB5857
FF1003 4.0.0.0.0.0.0.0.0.0 FF1003
FF1008 4.0.0.0.0.0.0.0.0.0 FF1008
FF1006 4.0.0.0.0.0.0.0.0.0 FF1006
FF1014 4.0.0.0.0.0.1.0.0.0 FF1014
FF1011 4.0.0.0.0.0.1.2.0.0 FF1011
FF930 4.0.0.0.0.0.2.0.0.0 FF930
FF1017 4.0.0.0.0.0.1.1.0.0 FF1017
SB98 2.0.8.1.0.0.0.0.0.0 SB98
SB11 2.0.15.0.2.0.0.0.0.0 SB11
SB59 2.0.37.0.0.0.0.0.0.0 SB59
SB2110 2.0.0.1.0.0.0.0.0.0 SB2110
SB203 2.1.47.0.0.0.0.0.0.0 SB203
SB610 2.1.38.0.0.0.0.0.0.0 SB610
SB30 2.1.22.0.0.0.0.0.0.0 SB30
SB4697 2.1.23.0.0.0.0.0.0.0 SB4697
SB164 2.1.26.0.1.0.0.0.0.0 SB164
SB579 1.0.126.0.0.0.0.0.0.0 SB579
SB48 1.0.65.0.0.0.0.0.0.0 SB48
SB1 1.0.72.1.0.0.0.0.0.0 SB1
SB4767 1.0.6.0.0.0.0.0.0.0 SB4767
SB94 1.1.5.0.0.0.0.0.0.0 SB94
SB5439 1.1.3.0.0.0.0.0.0.0 SB5439
SB5544 1.1.1.0.0.0.0.0.0.0 SB5544
SB5531 1.1.0.0.0.0.0.0.0.0 SB5531
SB5387 1.1.8.0.0.0.0.0.0.0 SB5387
SB5610 1.1.9.0.0.0.0.0.0.0 SB5610
Kp1
Kp6
Kp7
Kp2
Kp4
Kp3
Kp5
Tree scale: 0.01

Figure 6

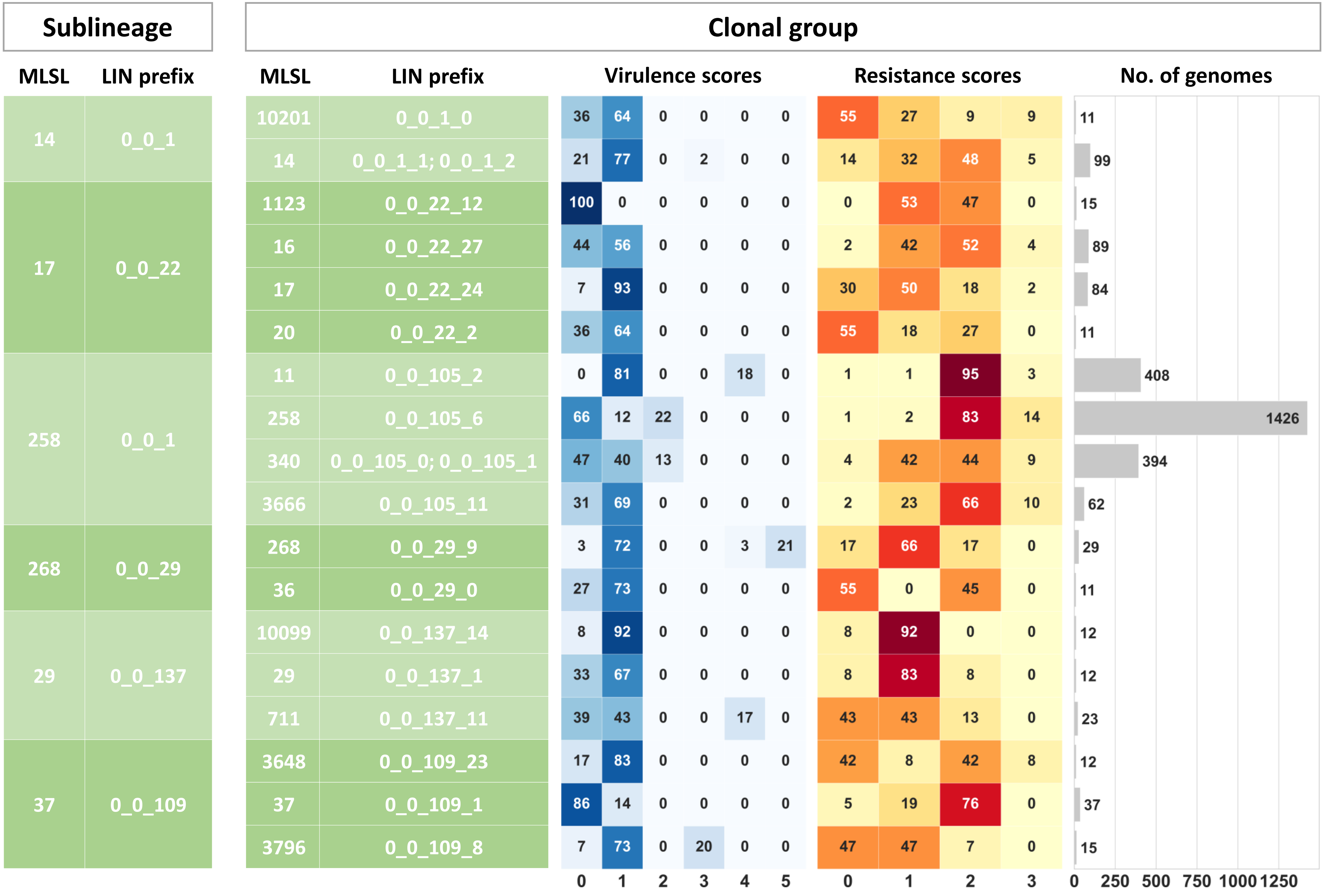

Sublineage		Clonal group												
MLSL	LIN prefix	MLSL	LIN prefix	Virulence scores						Resistance scores				No. of genomes
				0	1	2	3	4	5	0	1	2	3	
14	0_0_1	10201	0_0_1_0	36	64	0	0	0	0	55	27	9	9	11
		14	0_0_1_1; 0_0_1_2	21	77	0	2	0	0	14	32	48	5	99
17	0_0_22	1123	0_0_22_12	100	0	0	0	0	0	0	53	47	0	15
		16	0_0_22_27	44	56	0	0	0	0	2	42	52	4	89
		17	0_0_22_24	7	93	0	0	0	0	30	50	18	2	84
		20	0_0_22_2	36	64	0	0	0	0	55	18	27	0	11
258	0_0_1	11	0_0_105_2	0	81	0	0	18	0	1	1	95	3	408
		258	0_0_105_6	66	12	22	0	0	0	1	2	83	14	1426
		340	0_0_105_0; 0_0_105_1	47	40	13	0	0	0	4	42	44	9	394
		3666	0_0_105_11	31	69	0	0	0	0	2	23	66	10	62
268	0_0_29	268	0_0_29_9	3	72	0	0	3	21	17	66	17	0	29
		36	0_0_29_0	27	73	0	0	0	0	55	0	45	0	11
29	0_0_137	10099	0_0_137_14	8	92	0	0	0	0	8	92	0	0	12
		29	0_0_137_1	33	67	0	0	0	0	8	83	8	0	12
		711	0_0_137_11	39	43	0	0	17	0	43	43	13	0	23
37	0_0_109	3648	0_0_109_23	17	83	0	0	0	0	42	8	42	8	12
		37	0_0_109_1	86	14	0	0	0	0	5	19	76	0	37
		3796	0_0_109_8	7	73	0	20	0	0	47	47	7	0	15

Table 1. Genome dataset phylogroup breakdown, quality assessment and diversity

Taxonomic Designation	Phylogroup	Initial No. Genomes	No. QC-filtered	No. after applying filters	No. of hybrids	No. of non-hybrid genomes	No. Called alleles (mean, std)	No. of sequence types (ST)
K. pneumoniae subsp. *pneumoniae*	Kp1	6737	218 (3.2%)	6519 (90.6%)	43 (0.7%)	6476 (91.7%)	624.6 (3.6)	705
K. quasipneumoniae subsp. *quasipneumoniae*	Kp2	115	1 (0.9%)	114 (1.6%)	8 (7.0%)	106 (1.5%)	604.0 (2.5)	49
K. variicola subsp. *variicola*	Kp3	309	8 (2.6%)	301 (4.2%)	37 (12.3%)	264 (3.7%)	615.4 (3.3)	149
K. quasipneumoniae subsp. *similipneumoniae*	Kp4	230	6 (2.6%)	224 (3.1%)	50 (22.3%)	174 (2.5%)	607.4 (1.9)	64
K. variicola subsp. *tropica*	Kp5	19	0 (0.0%)	19 (0.3%)	0 (0.0%)	19 (0.3%)	611.7 (1.8)	13
K. quasivariicola	Kp6	13	2 (15.4%)	11 (0.2%)	0 (0.0%)	11 (0.2%)	602.9 (1.8)	8
K. africana	Kp7	10	0 (0.0%)	10 (0.1%)	0 (0.0%)	10 (0.1%)	606.3 (1.6)	4
Total		**7433**	**235**	**7198**	**138**	**7060**	**mean** **610.3 (2.36)**	**992**